Round-to-Flat Beam Transformation and Applications

Yine Sun
Accelerator System Division
Advanced Photon Source
Argonne Nation Lab.

International Workshop on Beam Cooling and Related Topics
Jefferson Lab, Newport News, Virginia, USA.
Sept. 28 – Oct. 2, 2015

Outline

- Introduction;
- Generation of magnetized electron bunches from a high-brightness RF photo-injector;
- Parameterization and measurements of the magnetized beam;
- Experimental demonstration of the removal of the angular momentum and the generation of a flat beam:
  - theory;
  - measurement method;
  - data analysis and results;
  - comparison with simulations.

Beam dynamics: three different regimes

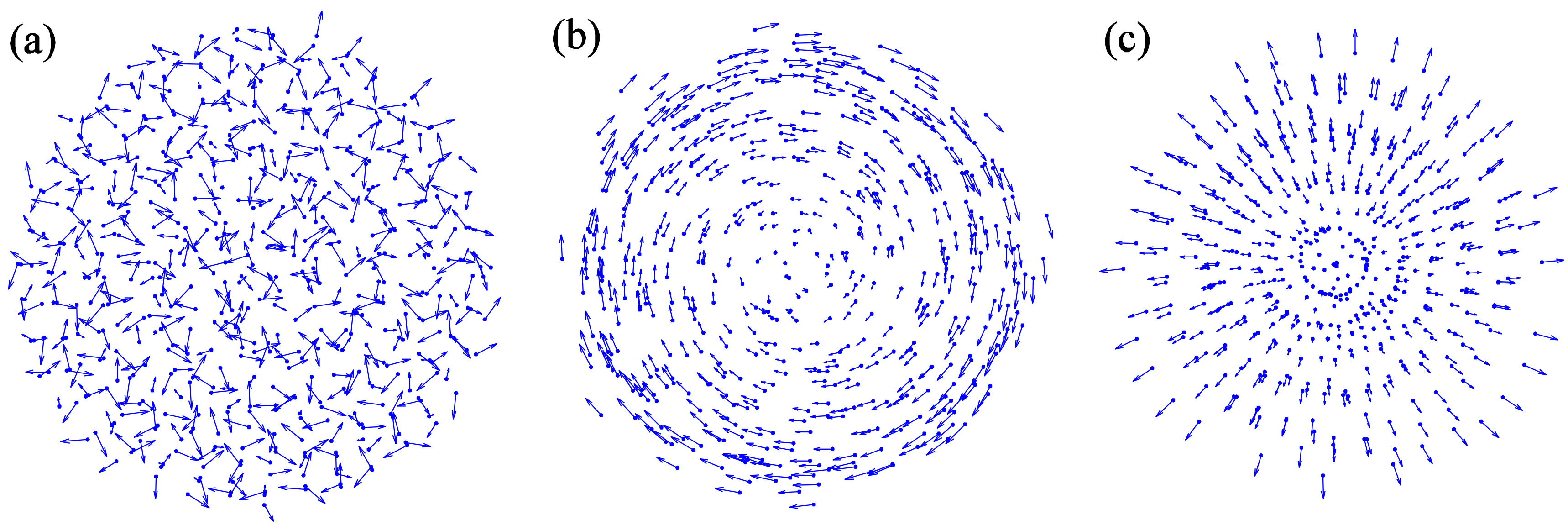

emittance

Magnetized
(canonical angular momentum)

space charge

envelope equation in a drift: $\sigma'' - \frac{\varepsilon^2}{\sigma^3} - \frac{L^2}{\sigma^3} - \frac{K}{4\sigma} = 0$ where $K = \frac{2I}{I_0 \beta^3 \gamma^3}$

is the generalized perveance.

Yine Sun, http://lss.fnal.gov/archive/thesis/2000/fermilab-thesis-2005-17.pdf

Applications of magnetized beam and flat beam

- Electron cooling for heavy ion: cooling interaction Time

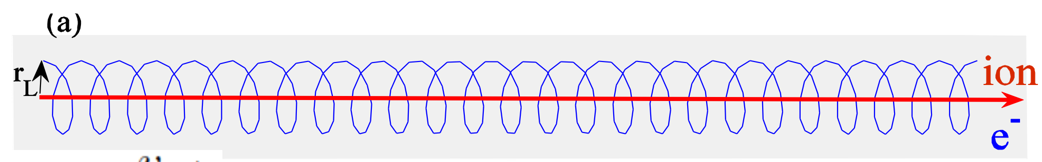

$$r_L = \frac{v_{e\perp}}{eB_z}$$

$$\tau_c^{mag} \approx \rho / \left(v_z^{ion} - v_z^{e} \right)$$

magnetized

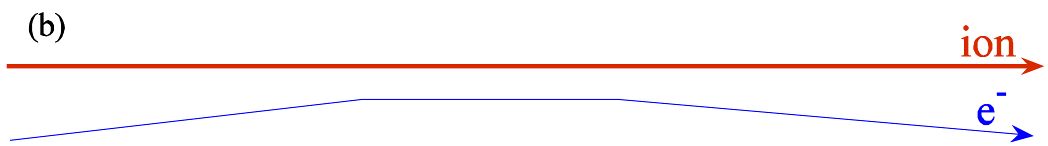

$$\tau_c^{free} \approx \rho / v_e^{\perp}$$

non - magnetized

- Flat beam for linear e^+e^- collider: reduce beamstrahlung

$$\text{luminosity} \propto \frac{1}{\sigma_x \sigma_y} \qquad \delta_{\mathrm{E}} \propto \frac{1}{(\sigma_x + \sigma_y)^2}$$

Applications of magnetized beam and flat beam

❑Flat beam for light sources

Radiators of planar geometry such in the Radiabeam-APS THz generation experiment carried out at the Injector Test Stand in APS/ANL.

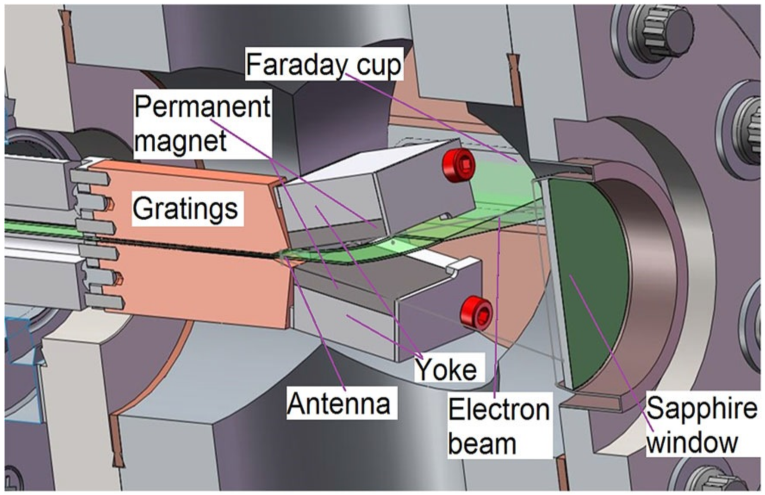

(a)

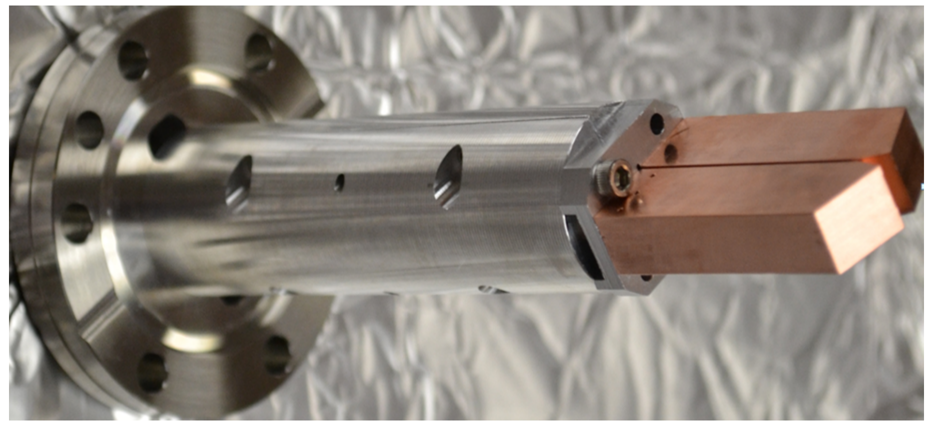

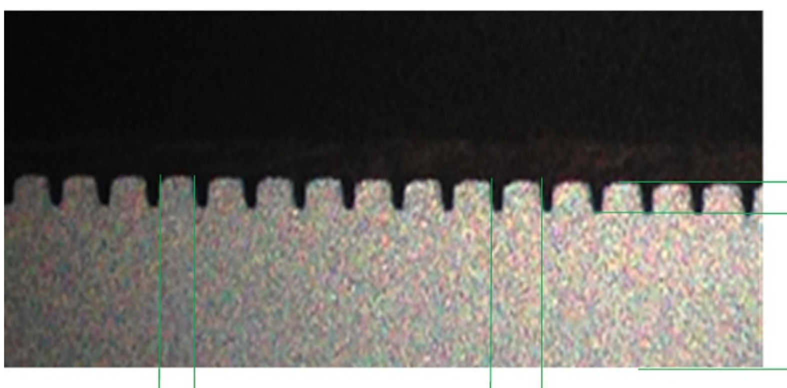

(b)

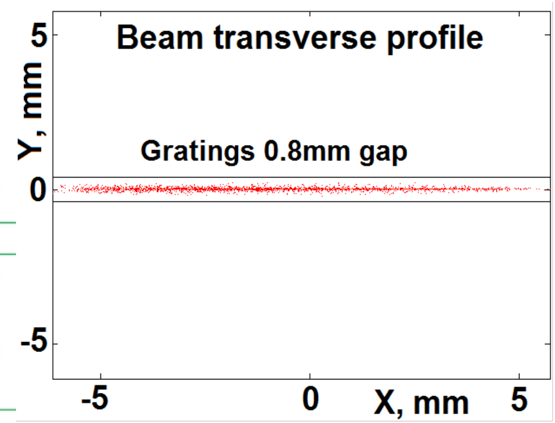

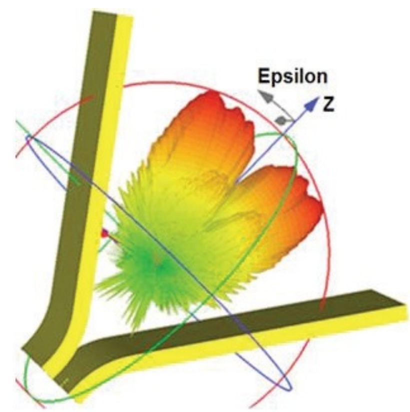

A. Smirnov, Phys. Rev. ST Accel. Beams 18, 090703 (2015).

Generation of magnetized electron beam From a high-brightness RF photo-injector

$$L = \gamma m r^2 \dot{\phi} + \frac{1}{2} e B_z r^2$$

On the cathode: $\langle L \rangle = e B_0 \sigma_c^2$

Solenoidal end field applies a torque to the beam. When B_z=0, canonical equals to the mechanical angular momentum.

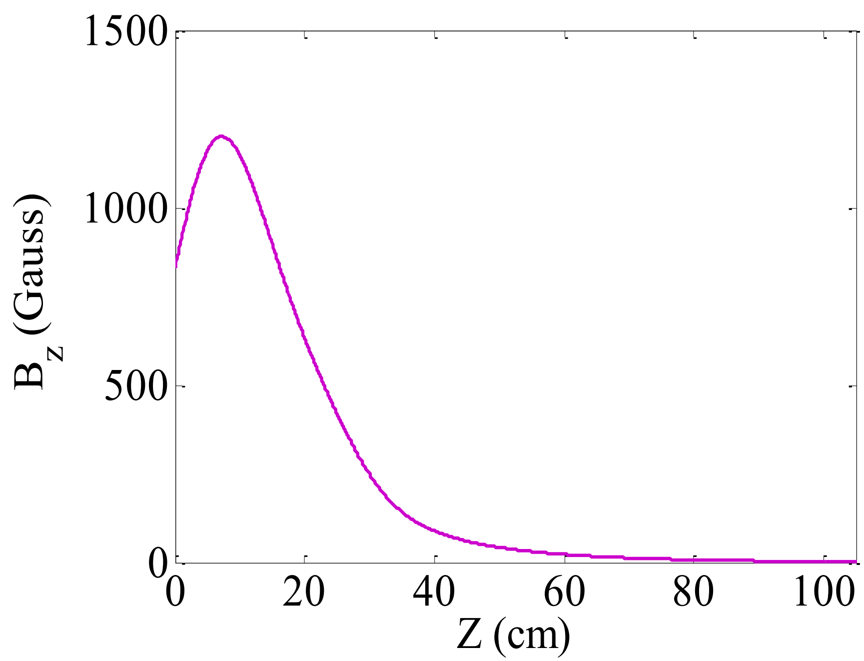

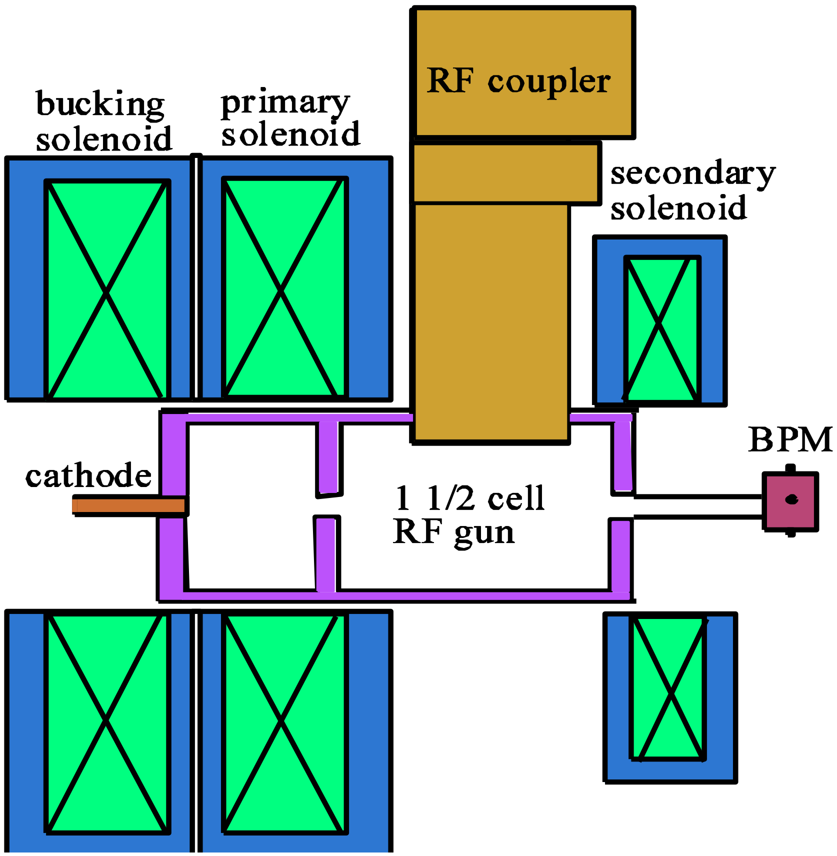

FNPL 1.625-cell RF gun, 1.3 GHz

Measurement of canonical angular momentum on the photocathode

$$\langle L \rangle = eB_0\sigma_c^2$$

B_0: B-field on cathode
σ_c :RMS beam size on cathode

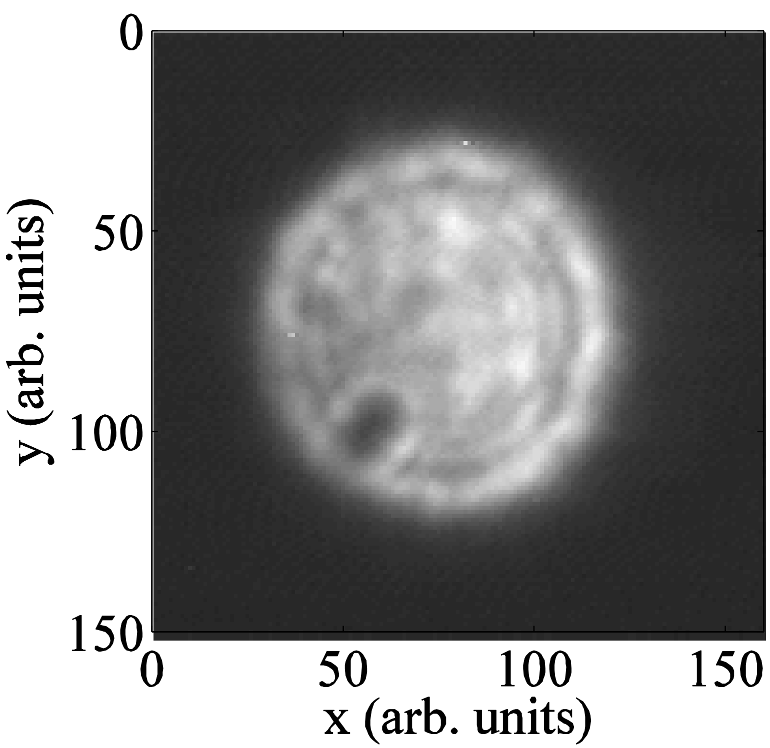

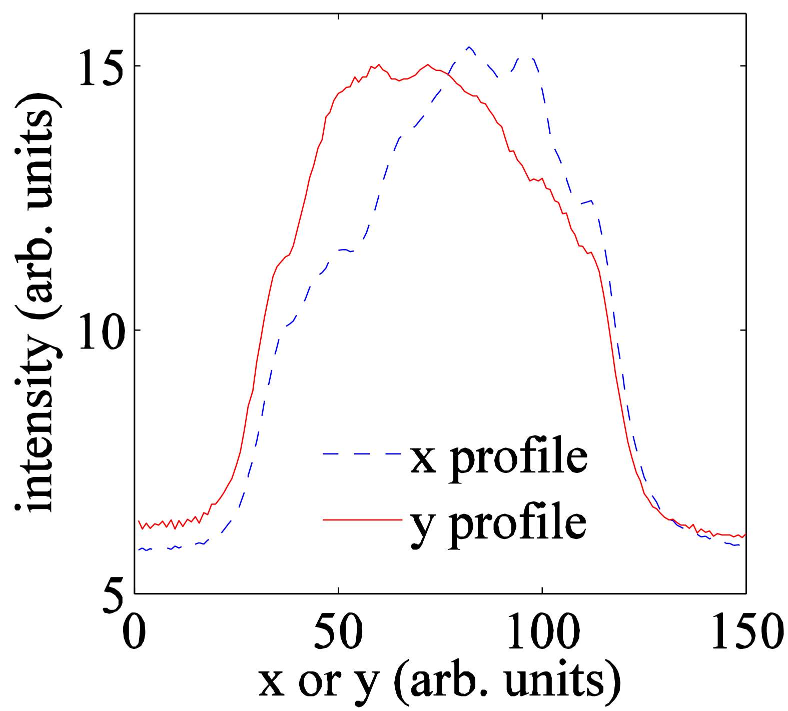

Measurement of mechanical angular momentum in a drift space

$$\boxed{\langle L \rangle = 2 p_z \frac{\sigma_1 \sigma_2 \sin\theta}{D}}$$

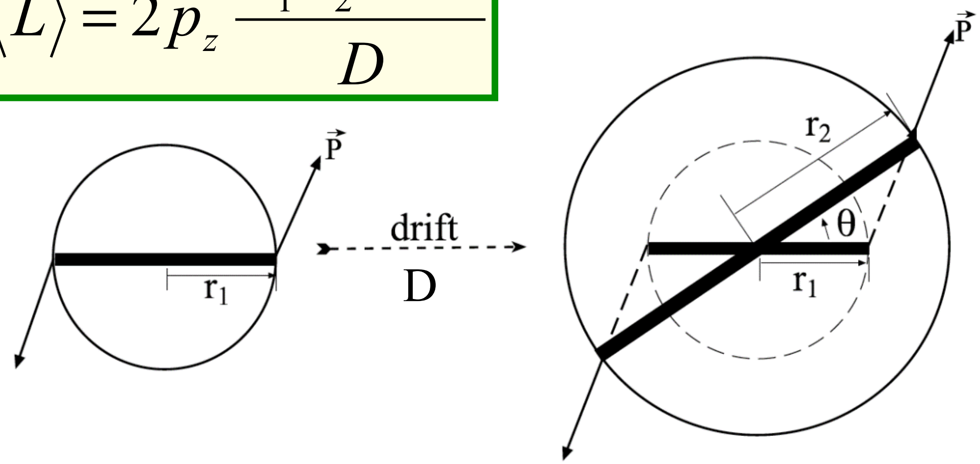

Y.-E Sun et al. Phys. Rev. ST Accel. Beams 7, 123501 (2004).

Measurement of mechanical angular momentum in a drift space

$$\langle L \rangle = 2 p_z \frac{\sigma_1 \sigma_2 \sin\theta}{D}$$

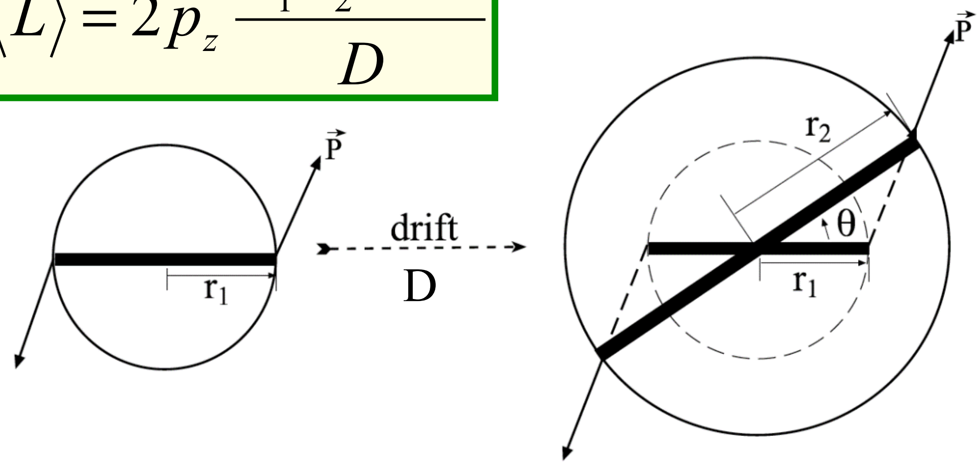

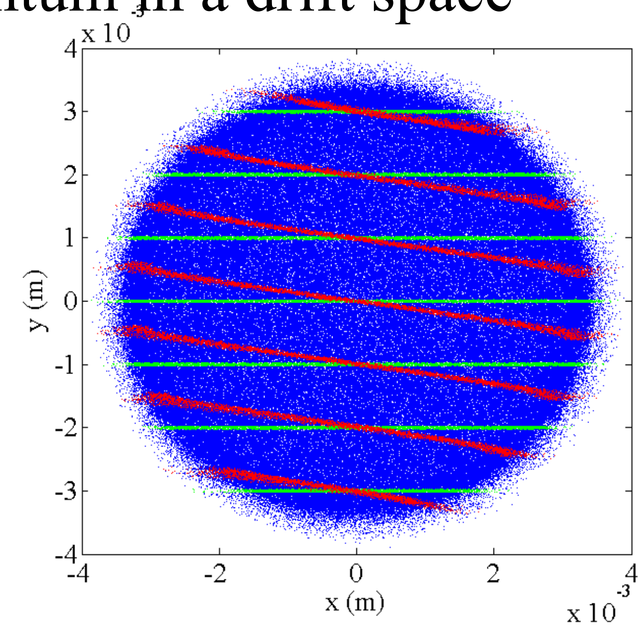

Y.-E Sun et al. Phys. Rev. ST Accel. Beams 7, 123501 (2004).

Measurement of mechanical angular momentum in a drift space

$$\boxed{\langle L \rangle = 2 p_z \frac{\sigma_1 \sigma_2 \sin\theta}{D}}$$

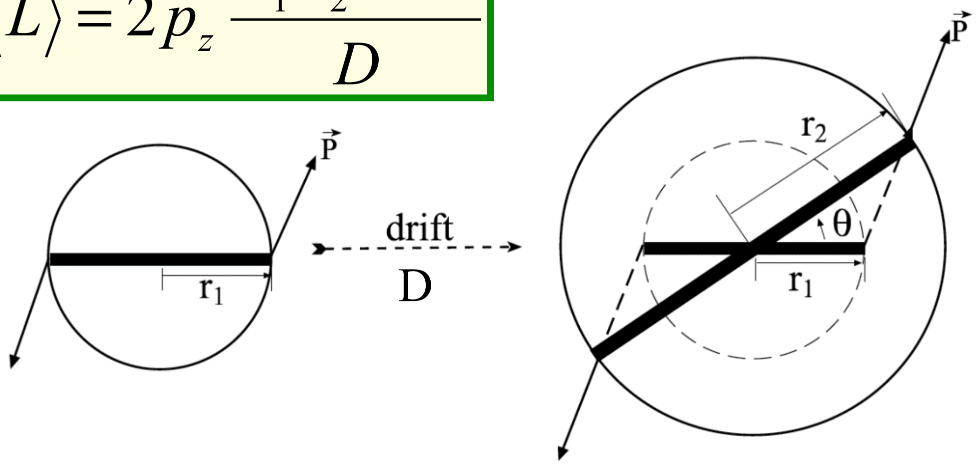

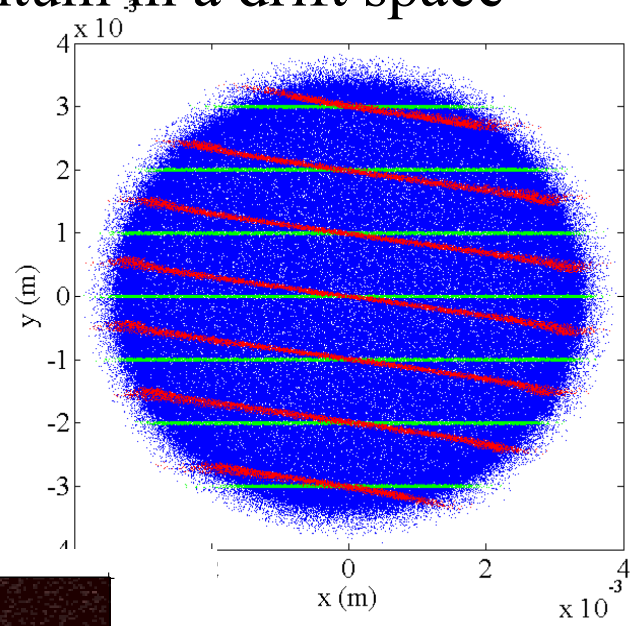

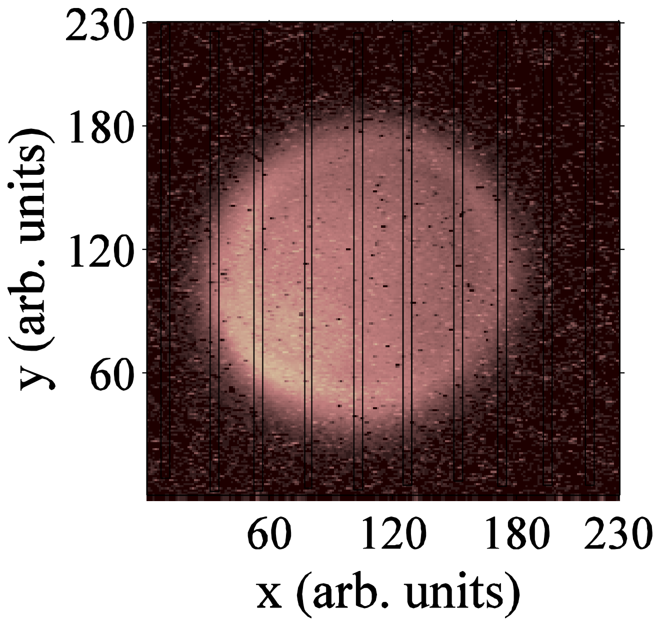

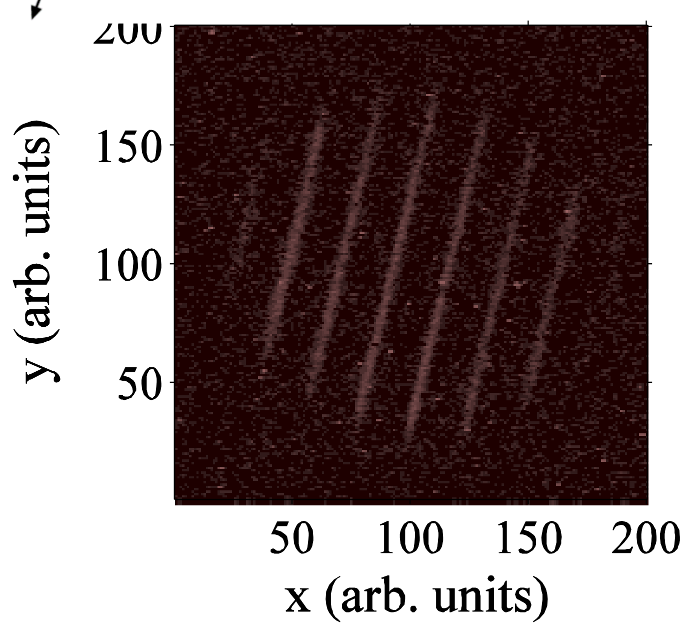

Y.-E Sun et al. Phys. Rev. ST Accel. Beams 7, 123501 (2004).

Measurement of rotation angle

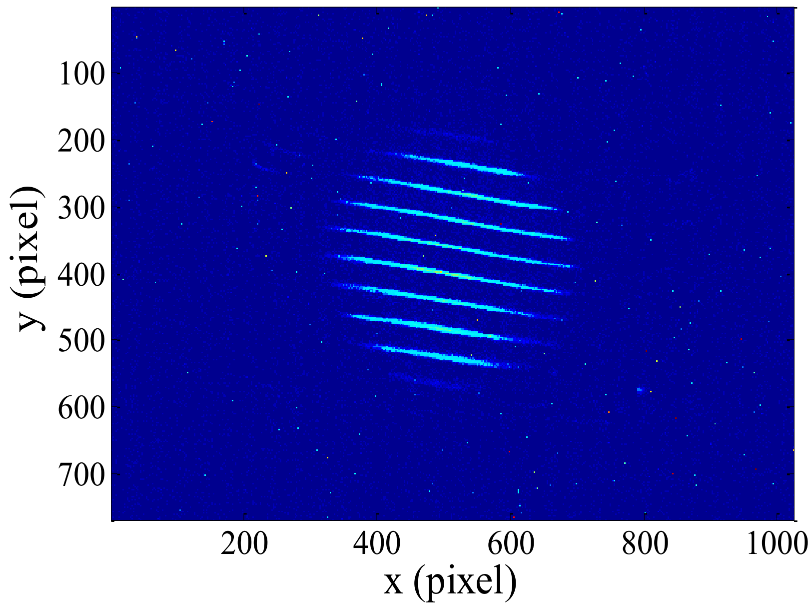

slit image

rotation of the slit image

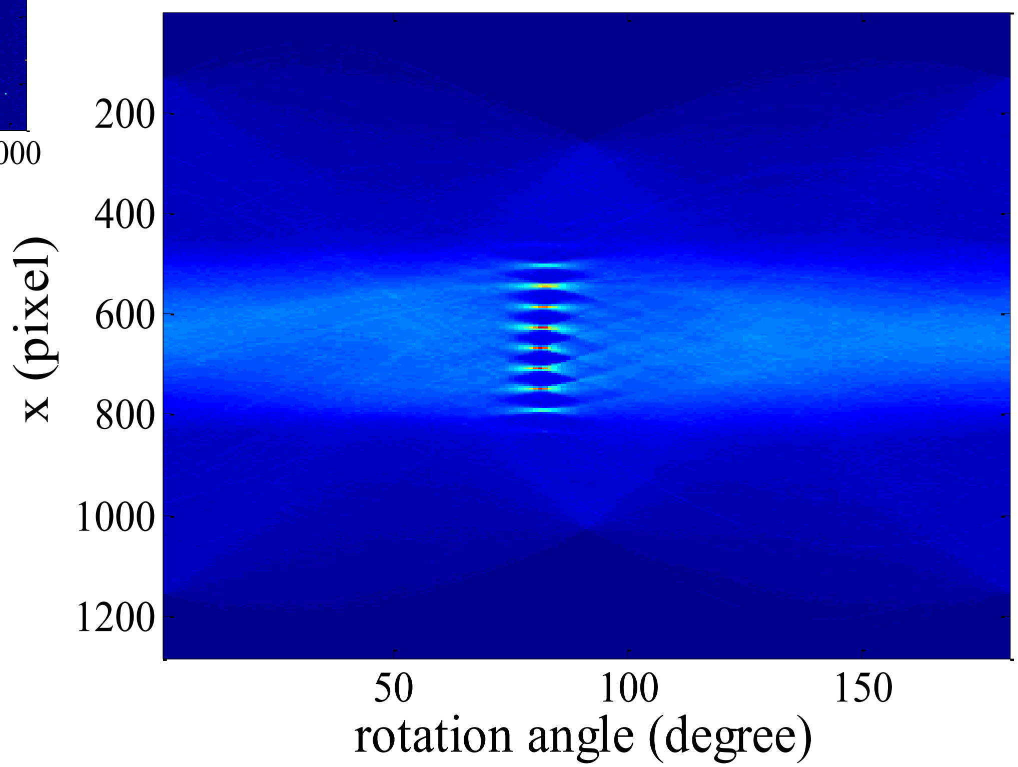

Measurement of mechanical angular momentum vs B-field

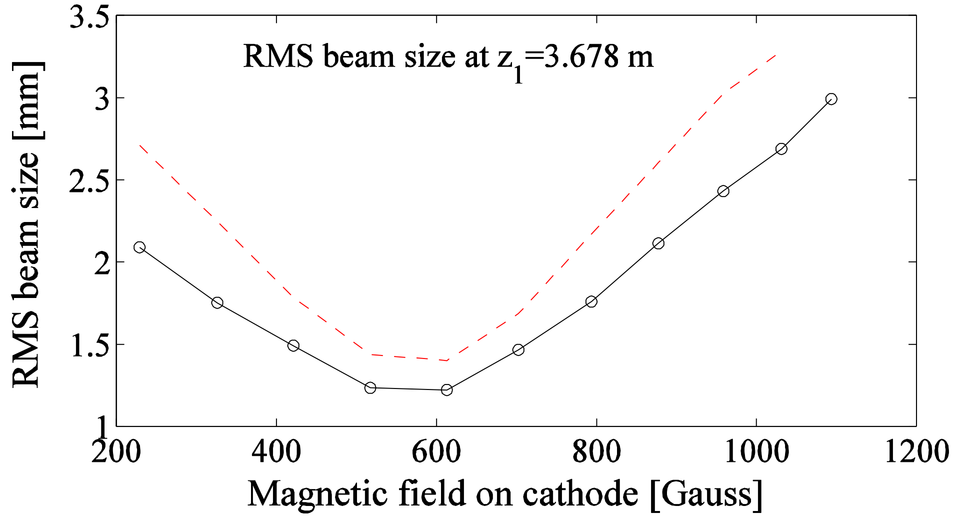

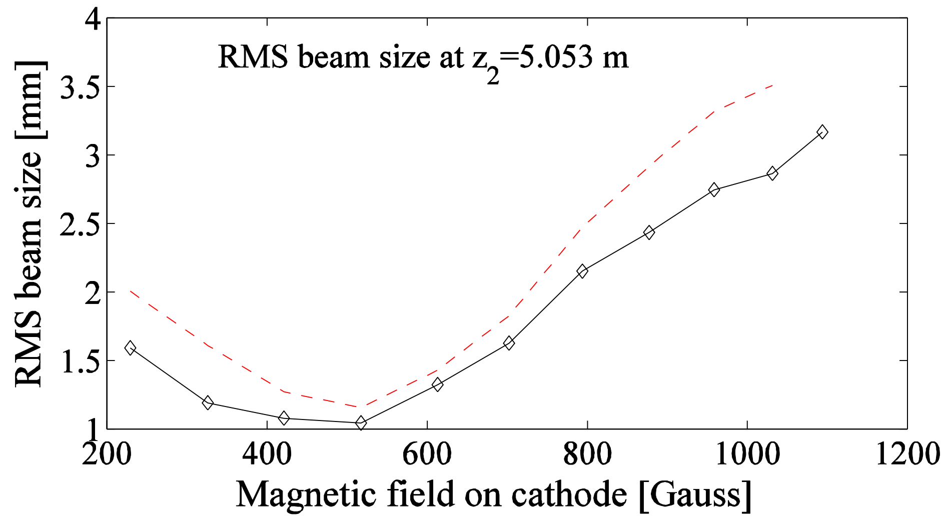

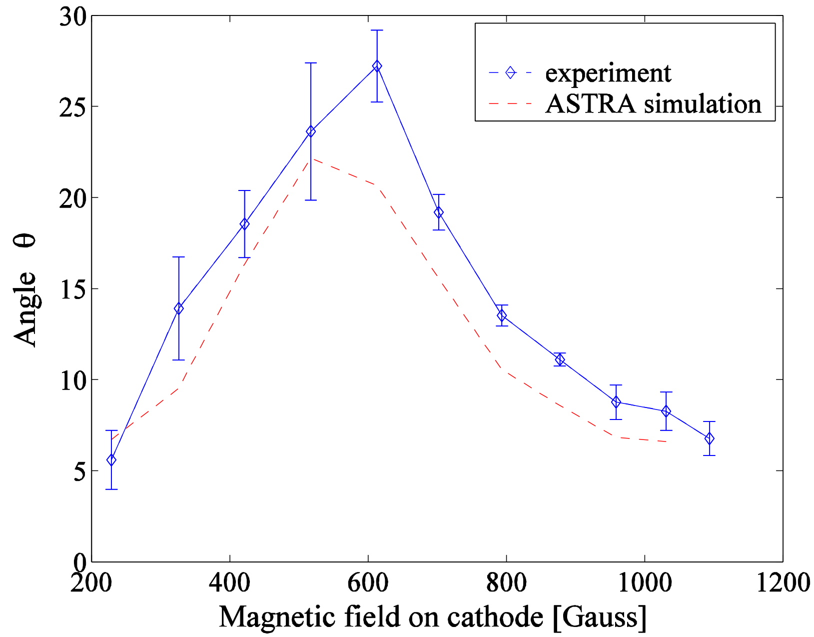

Demonstration of conservation of canonical angular momentum

as a function of magnetic field on cathode

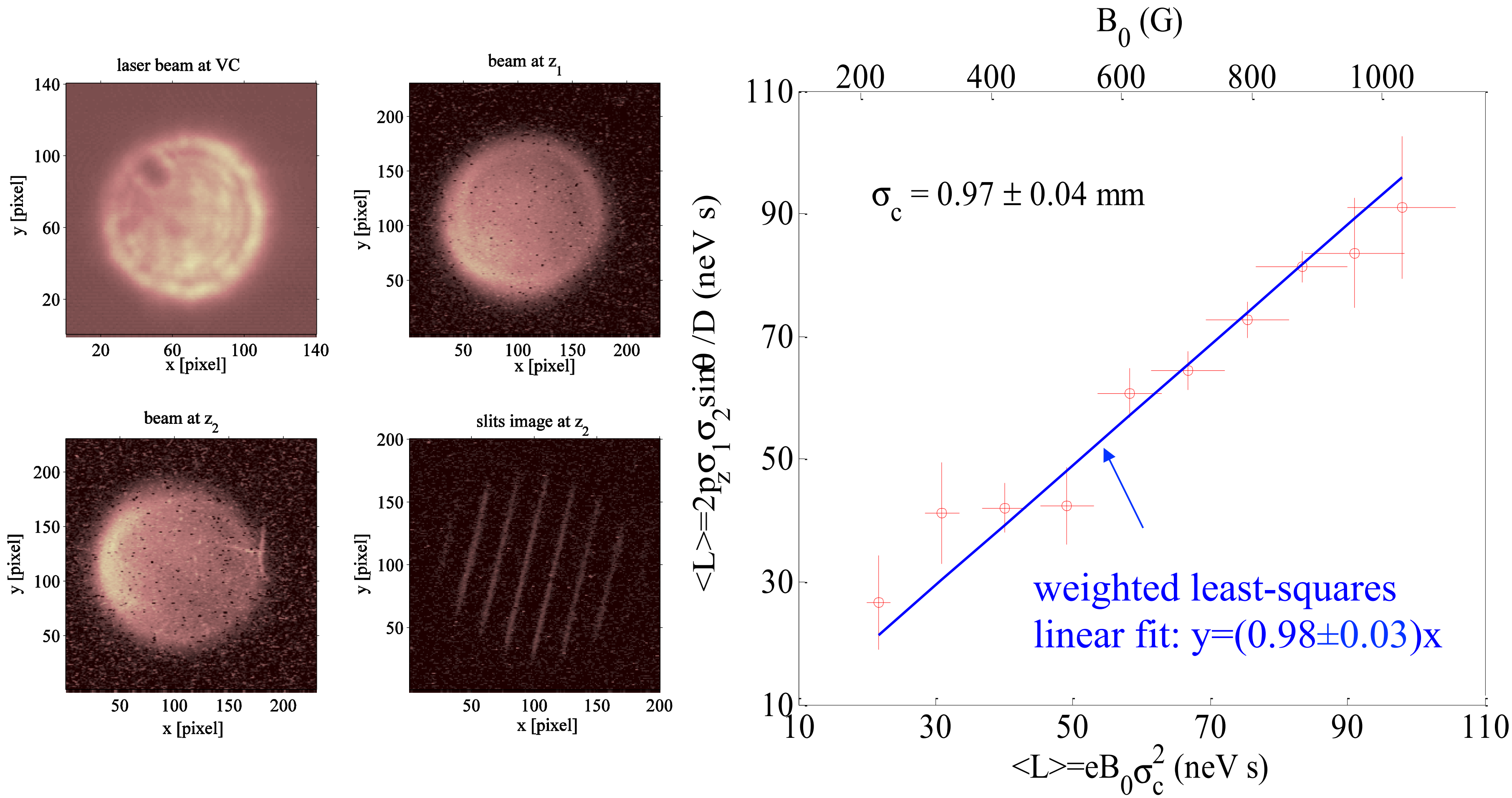

Parametric dependencies of angular momentum

- Angular momentum versus
  - beam longitudinal position z
  - bunch charge
  - beam size on the cathode

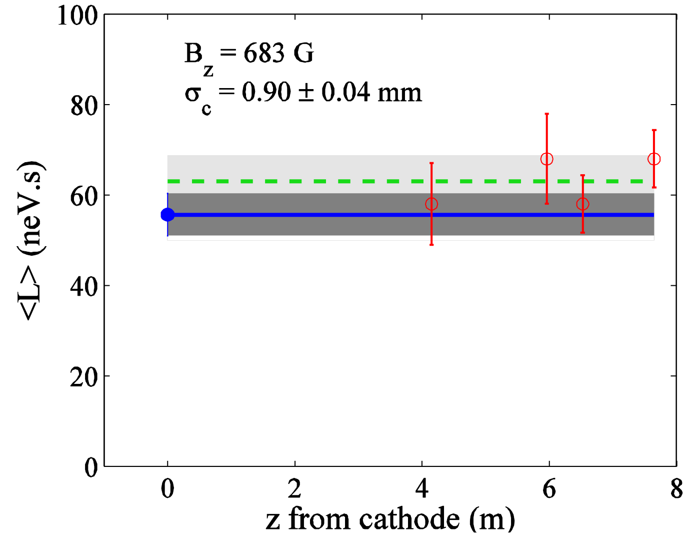

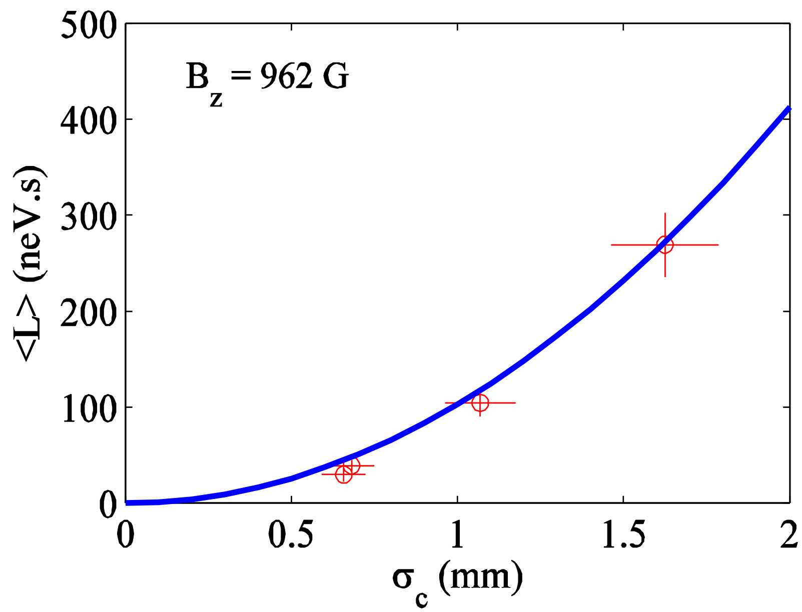

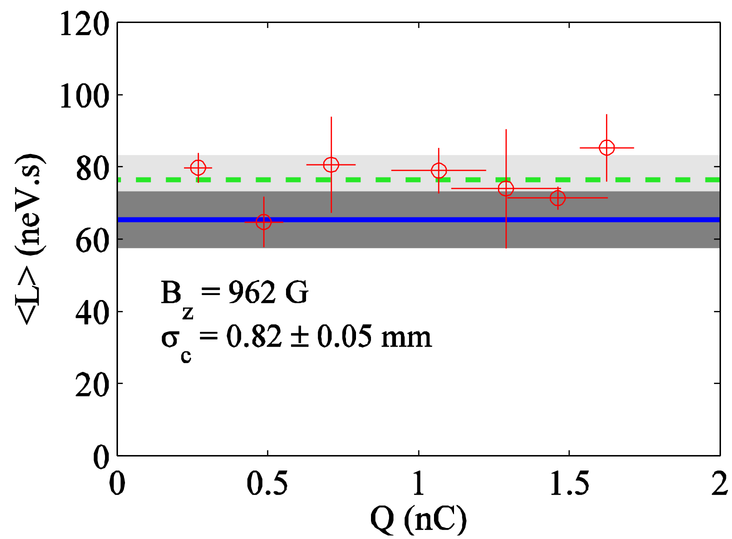

From magnetized beam to flat beam

Ya. Derbenev, "Adapting Optics for High Energy Electron Cooling", University of Michigan, UM-HE-98-04, Feb. 1998.
Ya. Derbenev, "Matched Electron Cooling", WEWAUD02, COOL'15.

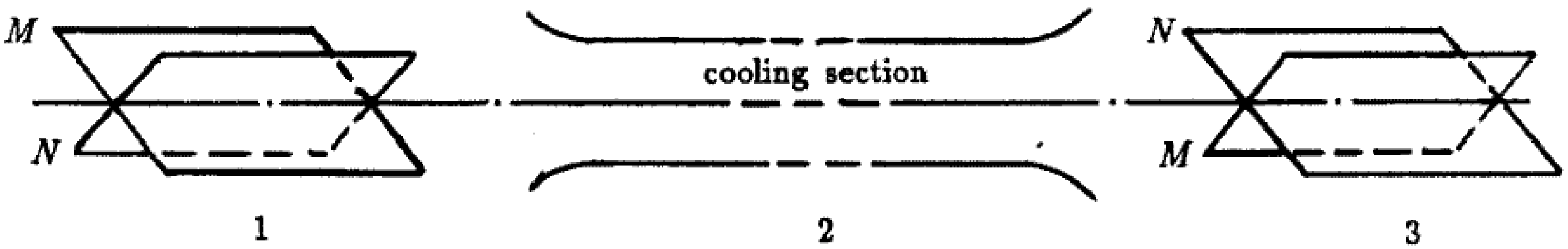

Figure 2.

Figure 2: Schematic of adapting optics for electron beam: 1) plane-vortex skew quadrupole transformer; 2) solenoid to stop the x-vortex; 3) vortex-plane transformer.

See also: A. Burov, S. Nagaitsev and Ya. Derbenev, Phys. Rev. E 66, 016503 (2002).

From magnetized beam to flat beam

Ya. Derbenev, “Adapting Optics for High Energy Electron Cooling”, University of Michigan, UM-HE-98-04, Feb. 1998.
Ya. Derbenev, “Matched Electron Cooling”, WEWAUD02, COOL’15.

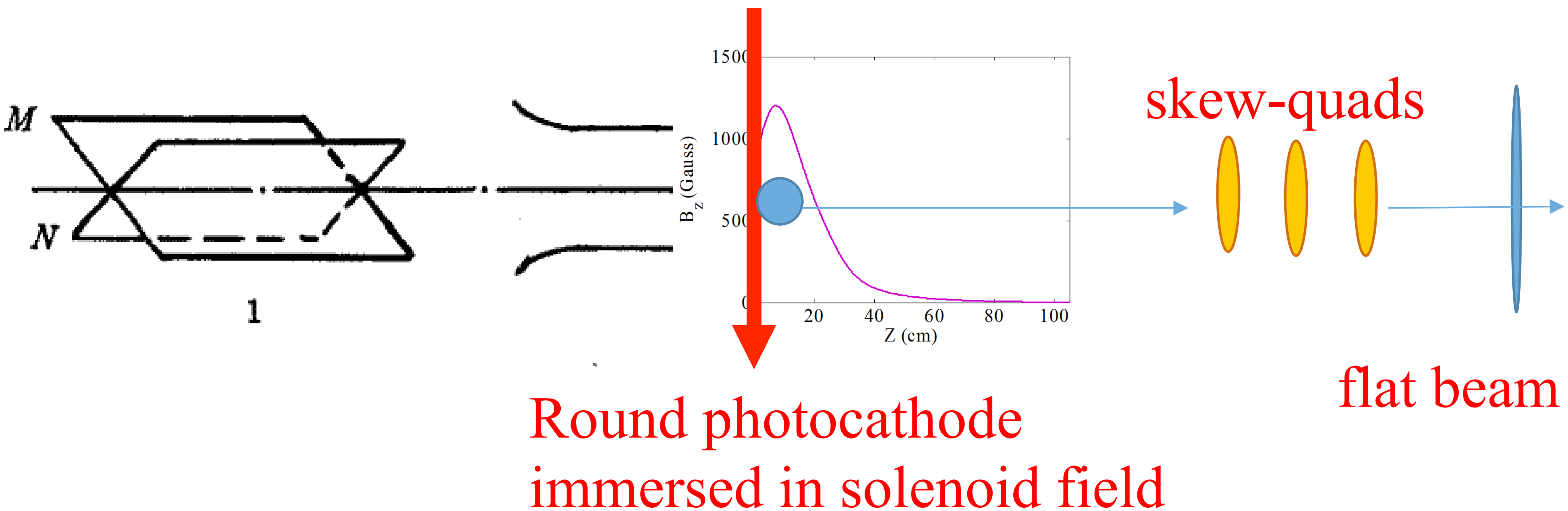

Figure 2: Schematic of adapting optics for electron beam: 1) plane-vortex skew quadrupole transformer; 2) solenoid to stop the x-vortex; 3) vortex-plane transformer.

See also: A. Burov, S. Nagaitsev and Ya. Derbenev, Phys. Rev. E 66, 016503 (2002).

Fermilab/NICADD Photoinjector Lab. (FNPL)

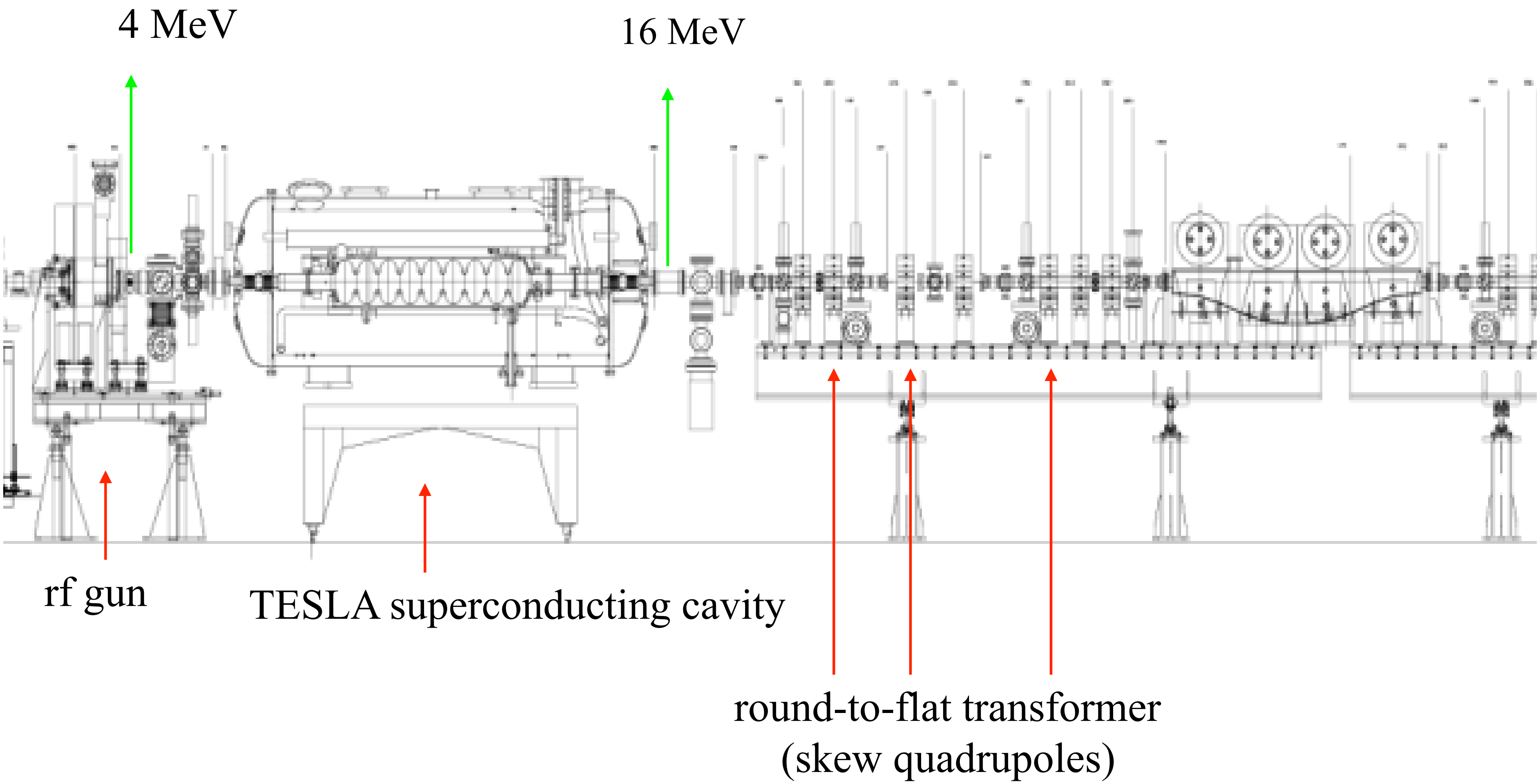

Round-to-flat beam transformation using skew quadrupoles

Flat beam: large transverse emittance ratio, zero average angular momentum.

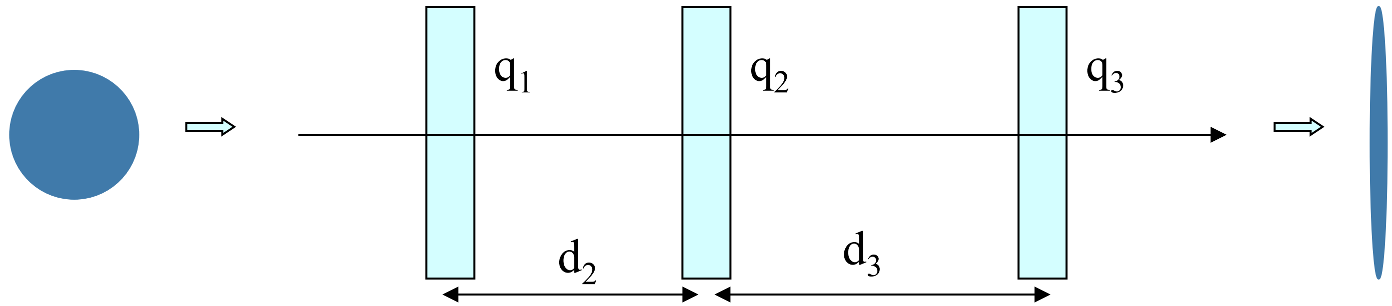

$$\langle \tau \rangle_{total} = 2 \cdot \sum q_i \langle x_i \, y_i \rangle$$

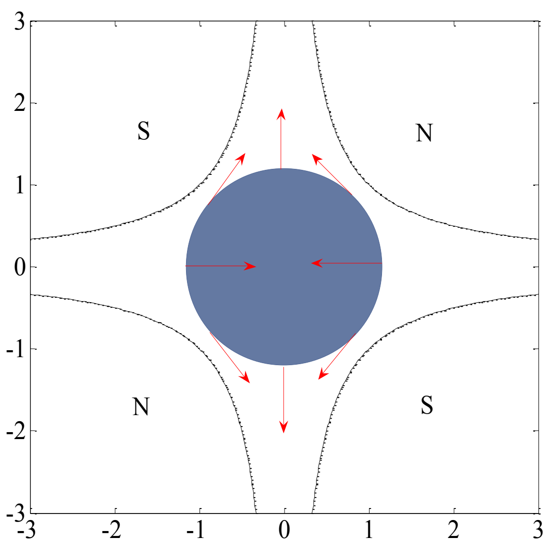

Two sets of solutions:

$$q_1 = \pm \sqrt{\frac{-d_2 S_{11} + S_{12} - d_2 d_T S_{21} + d_T S_{22}}{d_2 d_T S_{12}}}$$

$$q_2 = -\frac{S_{12} + d_T S_{22}}{d_2 d_3 (1 + S_{12} q_1)}$$

(D. Edwards)

$$q_3 = -\frac{q_1 + q_2 + d_2 S_{11} q_1 q_2 + S_{21}}{1 + (d_T q_1 + d_3 q_2) S_{11} + d_2 d_3 q_2 (S_{21} + q_1)}$$

Round-to-flat beam transformation

$$\Sigma_{round} = \begin{bmatrix} \varepsilon_{eff}\beta & 0 & 0 & L \\ 0 & \varepsilon_{eff}/\beta & -L & 0 \\ 0 & -L & \varepsilon_{eff}\beta & 0 \\ L & 0 & 0 & \varepsilon_{eff}/\beta \end{bmatrix}$$

General form of a round beam at beam waist location

(K.-J. Kim)

$$\varepsilon_{eff} = \sqrt{\varepsilon_u{}^2 + L^2}$$

uncorrelated emittance

"normalized" canonical angular momentum

$$\Sigma_{flat} = M\,\Sigma_{round}\,\tilde{M}$$

Transfer matrix
of the round-to-flat
beam transformer
(skew quadrupoles)

Flat beam emittances given by:

$$\varepsilon_{\pm} = \sqrt{\varepsilon_u{}^2 + L^2} \pm L$$

$$\Sigma_{flat} = \begin{bmatrix} \varepsilon_{-}\beta & 0 & 0 & 0 \\ 0 & \varepsilon_{-}/\beta & 0 & 0 \\ 0 & 0 & \varepsilon_{+}\beta & 0 \\ 0 & 0 & 0 & \varepsilon_{+}/\beta \end{bmatrix}$$

e.g. L=20 mm mrad, ε_u=1 mm mrad
ε_+=47 mm mrad; ε_-=0.02 mm mrad

Position and velocity snap shots at the entrance/exit of the transformer (ASTRA simulations)

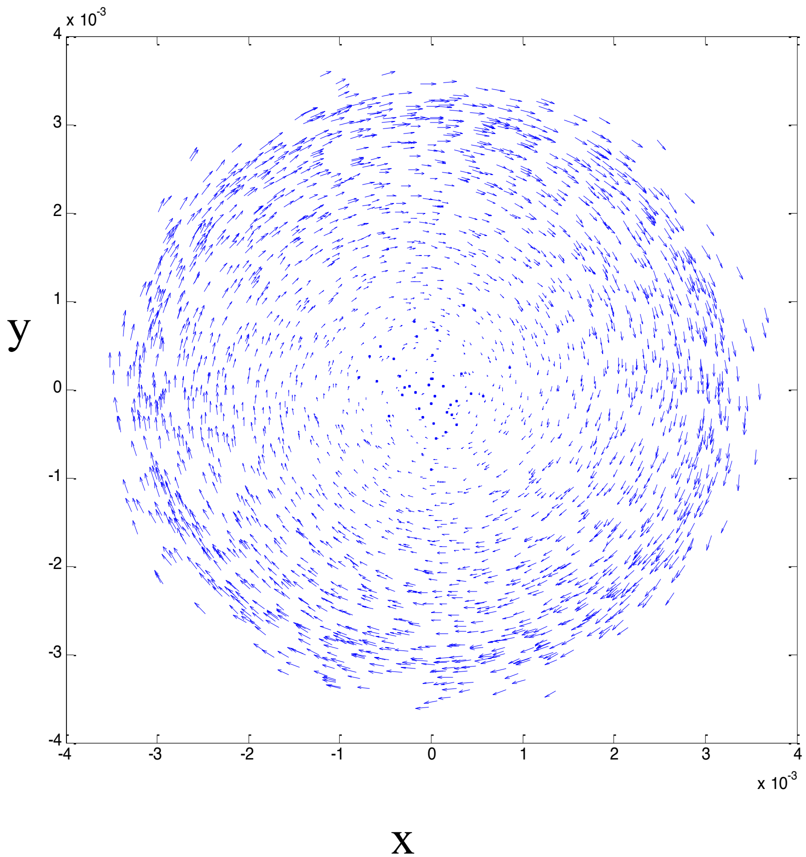

Round beam

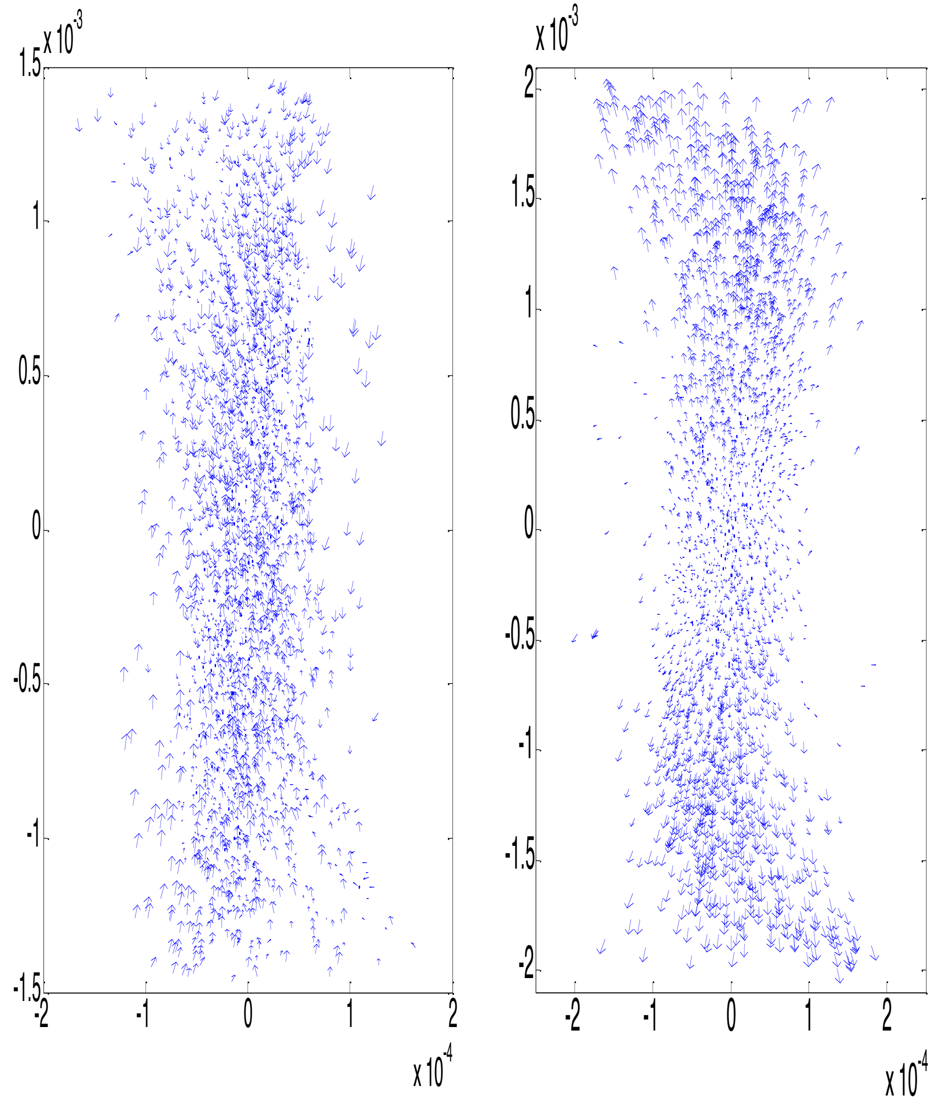

flat beam

Beam evolution through the transformer for the first solution

Right before 1st quad

Right after 1st quad

Right before 2nd Quad

Right after 2nd Quad

Right before 3rd quad

Right after 3rd quad

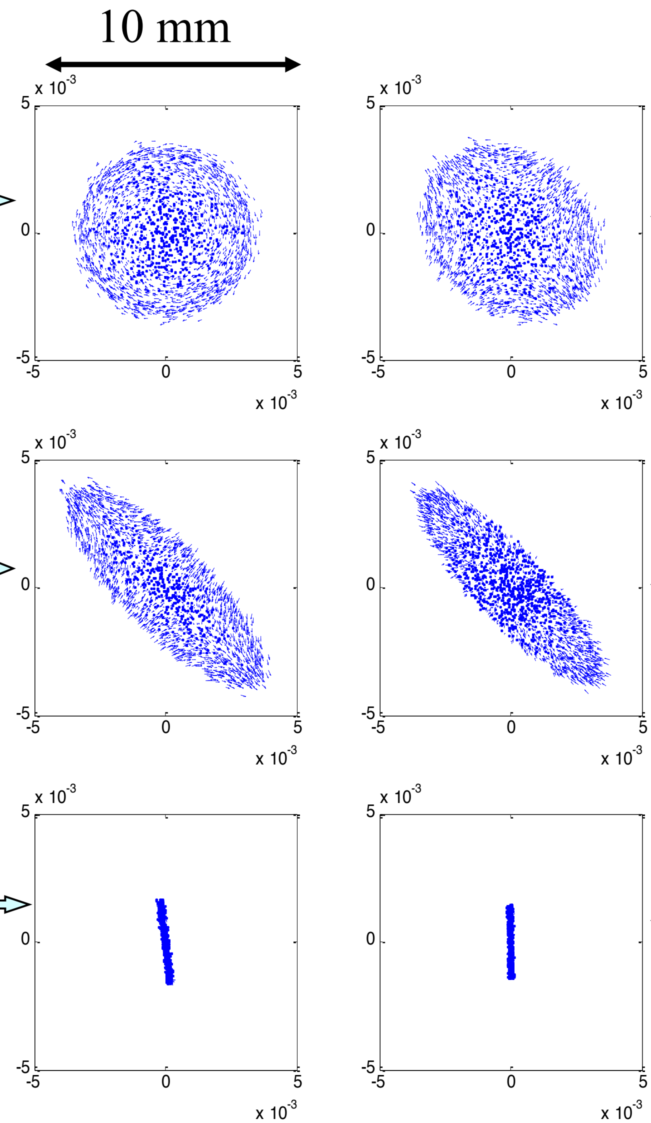

Removal of angular momentum and generating a flat beam

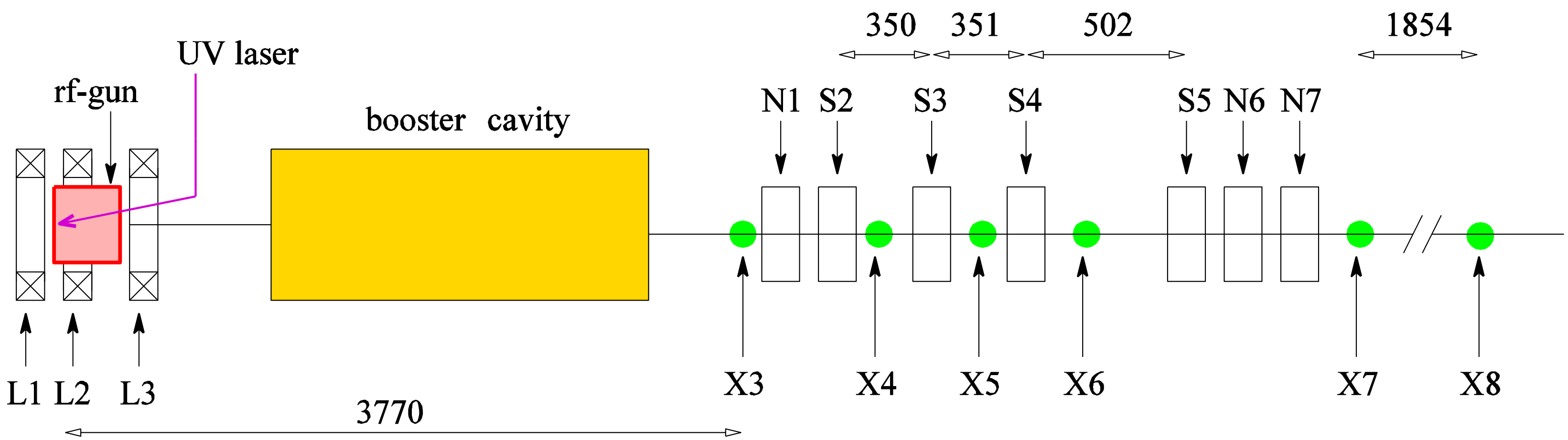

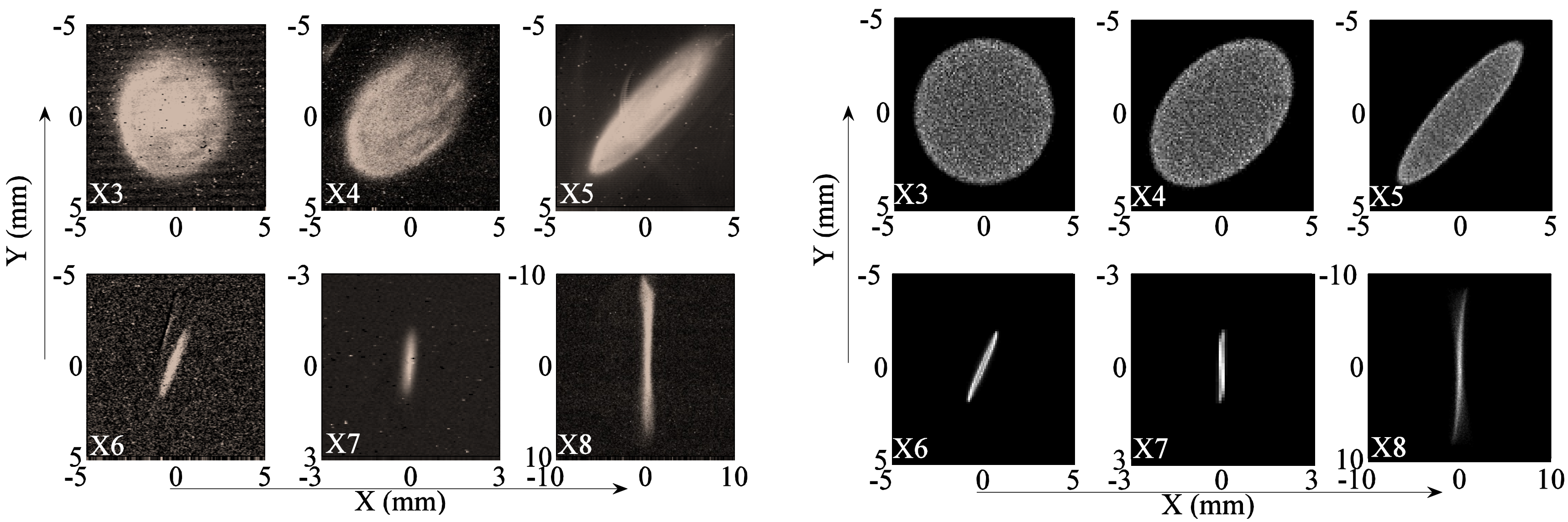

experiment

simulation

Flat beam measurements: beam images

Solenoid setting: main=195A, buck=0A, secondary=75A

σ = 0.97 mm, σ_t = 3 ps

E = 15.86 MeV Q = 0.51 ± 0.17 nC

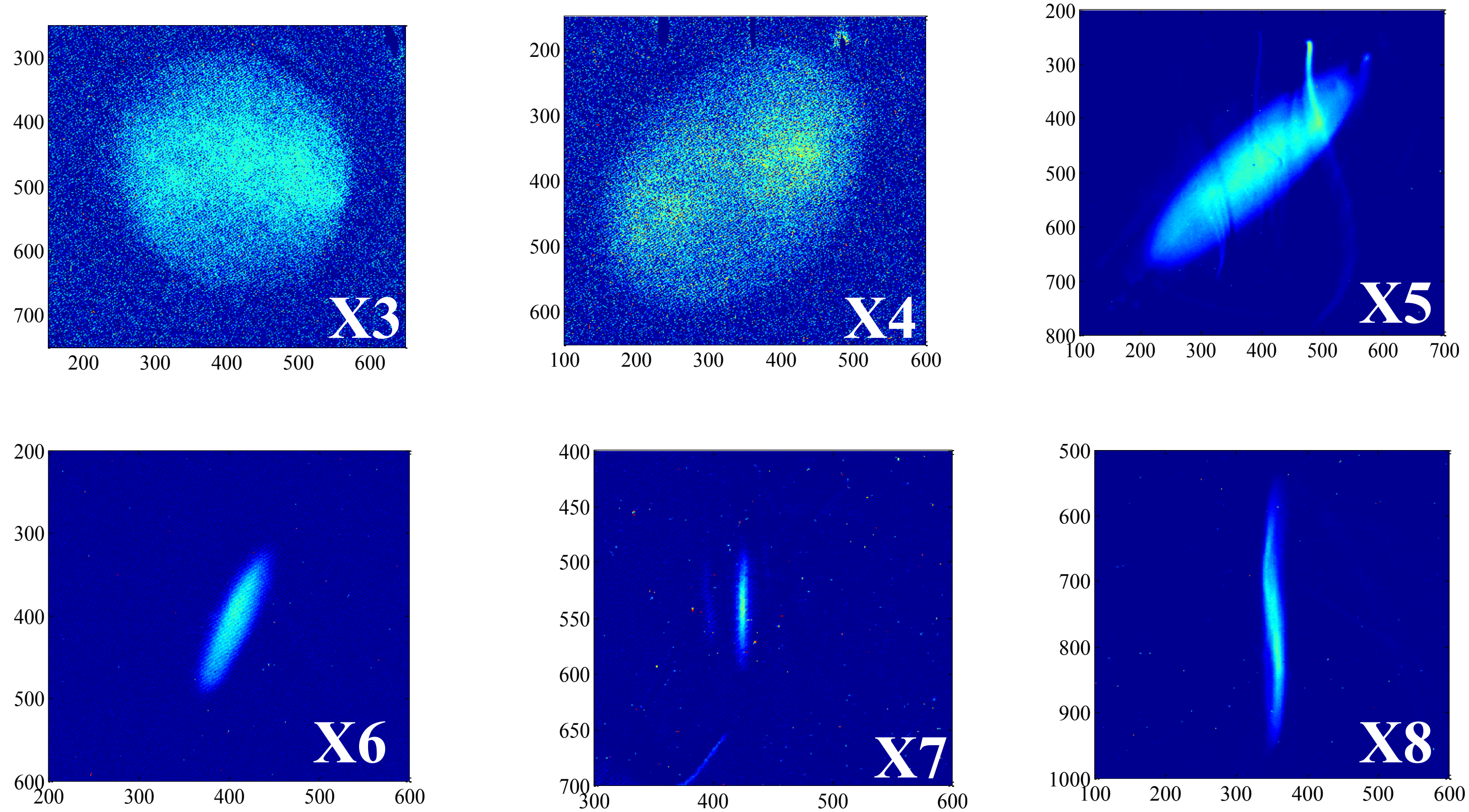

Flat beam experiment: emittance measurements

Solenoid setting:
main=190A,
buck=0A,
secondary=75A

Laser σ = 0.76 mm
σ_t = 3 ps

E = 15.8 MeV
Q = 0.50 ± 0.05 nC

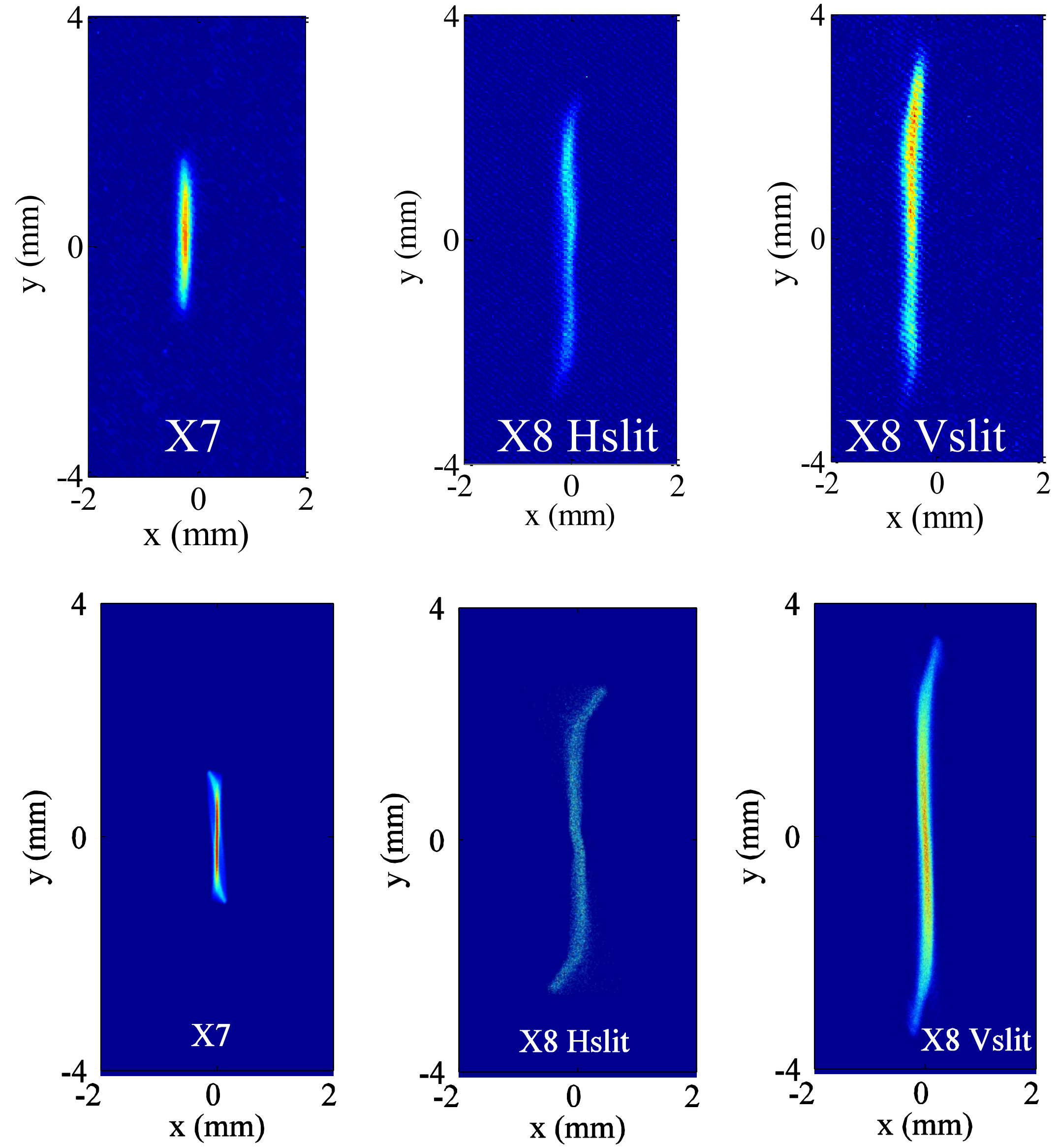

ASTRA Simulation with experimental conditions

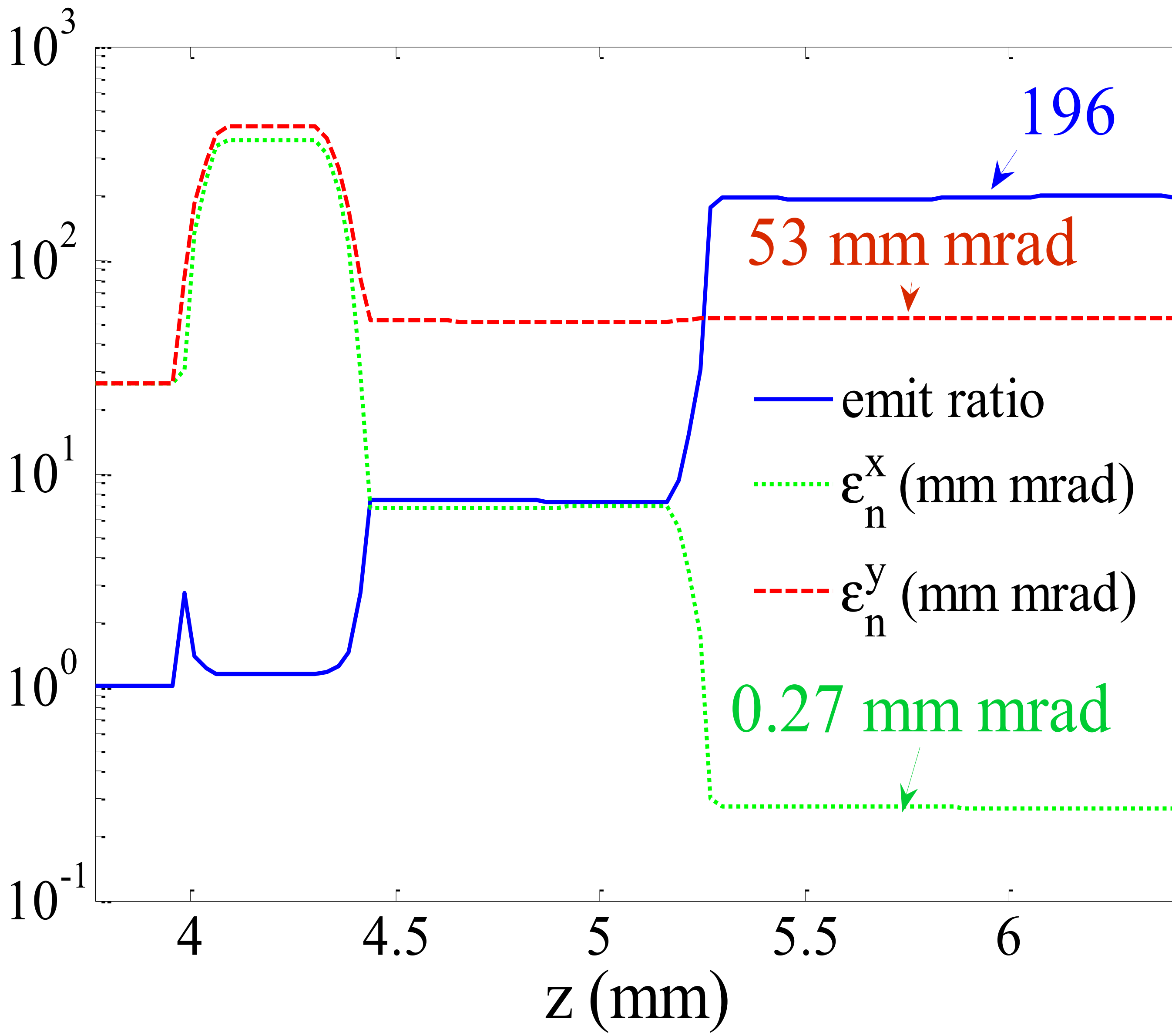

Experimental results compared with numerical simulations (0.5 nC)

Parameter	Experiment	Simulation	Unit
σ_x^{X7}	0.088 ± 0.01 (± 0.01)	0.058	mm
σ_y^{X7}	0.63 ± 0.01 (± 0.01)	0.77	mm
$\sigma_x^{X8,v}$	0.12 ± 0.01 (± 0.01)	0.11	mm
$\sigma_y^{X8,h}$	1.68 ± 0.09 (± 0.01)	1.50	mm
ε_n^x	$\boxed{0.41 \pm 0.06\ (\pm 0.02)}$	0.27	μm
ε_n^y	$\boxed{41.1 \pm 2.5\ (\pm 0.54)}$	53	μm
$\varepsilon_n^y/\varepsilon_n^x$	$\boxed{100.2 \pm 20.2\ (\pm 5.2)}$	196	

P. Piot, Y.-E Sun, K.-J. Kim, Phys. Rev. ST Accel. Beams 9, 031001 (2006).

Summary

- Magnetized photo-injector electron beams are generated and dependences on various parameters are studied. The angular-momentum-dominated electron beams are characterized;

- The magnetized electron beam is converted into a flat electron beam using a skew-quadrupole channel;

- The emittances of the flat beam are measured and at 0.5 nC, normalized emittance of **0.4 mm mrad** was measured; emittance ratio of **100** was achieved.